lajss.org
Latin American Journal of Solids and Structures
www.lajss.org

Research on the influence of inner liner on the Fragmentation Performance of Charge structure

Yongnan Li[a], Zhiyu Shao [a], Peizhuo Shi [a], Wang Yao [a], Yujing Li [a], Shuangxing Liu [a], Yongxiang Dong [a*]

[a]State Key Laboratory of Explosion Science and Technology, Beijing Institute of Technology; Beijing 100081, P. R. China.
Email:dongyongx@bit.edu.cn,3120220214@bit.edu.cn, 3120225101@bit.edu.cn,3120245151@bit.edu.cn

* Corresponding author

Abstract

To investigate the influence of inner liner on the fragmentation performance of prefabricated fragment charge structures, both experimental and numerical simulation studies were carried out on semi-prefabricated shell charge structures with liner, alongside numerical simulation studies on fully prefabricated fragment charge structures incorporating liner layers. The dynamic expansion and fragmentation processes, gas leakage behavior, and fragment velocity patterns of lined charge structures under explosion-driven were elucidated. Based on the experimental and numerical simulation findings of the semi-prefabricated shell charge structure with liner, the effects of liner material and thickness on the fragment velocity of the semi-prefabricated charge structure were explained. It was revealed that the thickness of the liner had a more significant effect on the fragment velocity than the material, exposing the staged acceleration characteristics of fragments and the role played by the liner in the fragment acceleration process. The numerical simulation study was conducted on the fully prefabricated column fragment charge structure with liner, and the acceleration characteristics of the explosion-driven fully prefabricated fragment charge structure were derived through the velocity-time history curve. The influence of the liner on the fully prefabricated fragment charge structure was also ascertained. Furthermore, the effects of liner material and thickness on the fragmentation velocity of semi-prefabricated explosive structures were investigated. It was found that the liner can increase both the gas leakage radius and fragmentation velocity. Notably, the velocity of the 10# steel liner charge structure can be increased by approximate 10% compared to unlined explosive structures, and the influence of liner material on fragmentation velocity is more significant than that of thickness.

Keywords

Liner; charge structure; explosion-driven; fragment velocity

Graphical Abstract

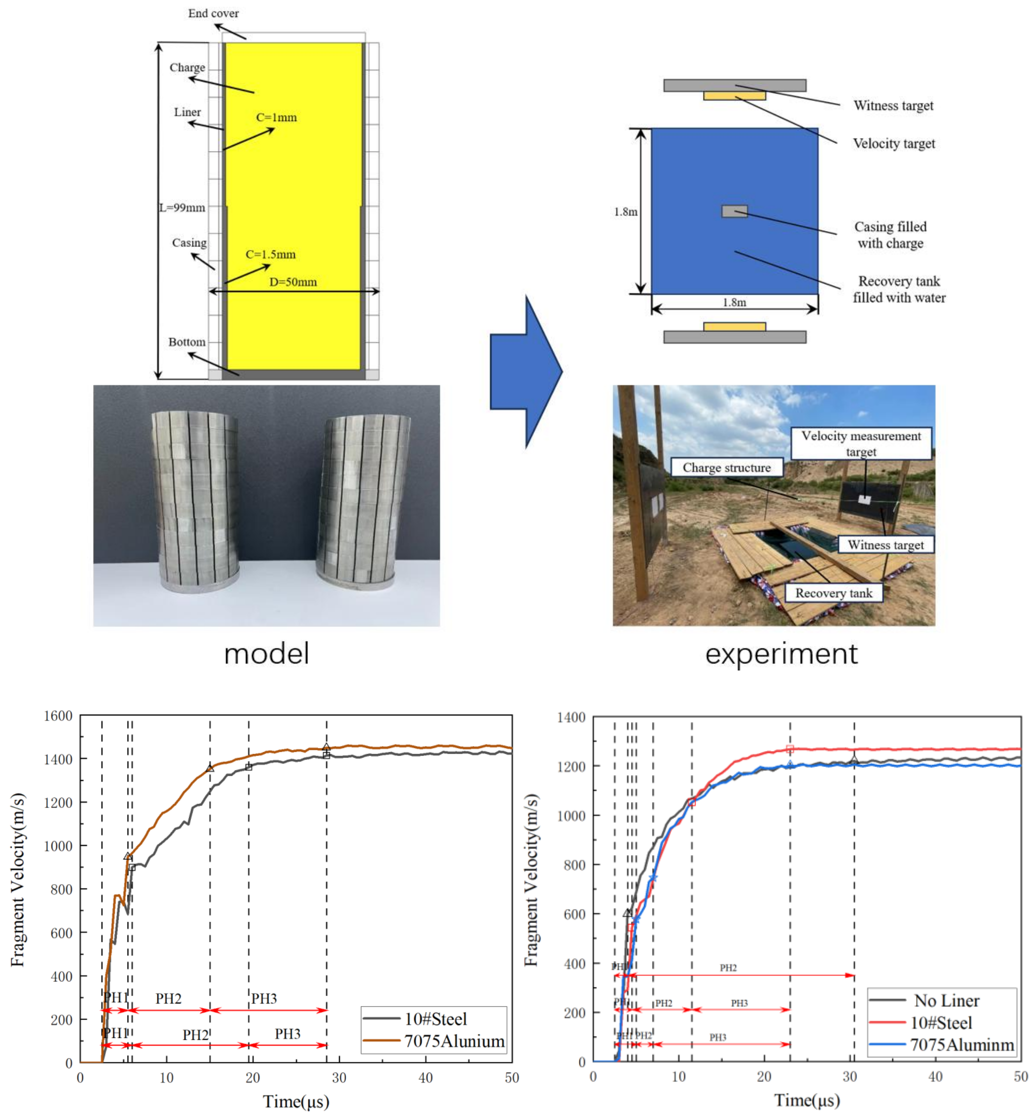

1 INTRODUCTION

After the detonation of cylindrical charges, the metal shell undergoes rapid acceleration driven by the detonation wave and internal detonation products, leading to substantial plastic deformation and fragmentation. In comparison to natural fragments, prefabricated fragments offer the advantage of precise control over fragment shape. Nevertheless, due to the early rupture of the shell during the explosion-driven process, which results in premature leakage of detonation products, the velocity of prefabricated fragments typically lags behind that of natural fragments. In the design of prefabricated shell charge structures, the incorporation of a liner becomes inevitable to ensure that the projectile can withstand high launch overloads and maintain structural integrity during assembly. This liner exerts a certain influence on the fragment characteristics of the prefabricated shell charge structure.

In the context of traditional unlined shells, Taylor(1963) was the first to consider the fracture behavior of continuous cylindrical shells, introducing strength and yield criteria, and establishing a model for the radial fracture process. However, Taylor's radial fracture theory is limited to low strain rates or thick-walled shells. Hoggatt and Recht(1968) enhanced Taylor's theory by incorporating a shear fracture mechanism. Zhang and Sun(1985) developed a model to predict the fracture radius and corresponding fracture velocity of cylindrical shells based on yield conditions, continuity equations, and motion equations.

Hutchinson et al.(2014) established a detonation product gas leakage model to address gas leakage and fragment acceleration following cylindrical shell rupture. This theory elucidates the escape of gas through debris gaps after the warhead shell fractures. Zhou(2020) formulated a theoretical model to describe the acceleration of a crushed cylindrical metal shell driven by explosion, taking into account the combined effects of shell crushing and gas leakage. The driving force on discrete fragments is adjusted based on changes in fragment area post-shell rupture and the subsequent reduction in gas pressure due to leakage. Yin(2014) divided the explosion-driven process into two phases: no leakage of explosive products and leakage, and established a calculation model for the velocity of cube fragments throughout the entire process. Li Yuan(2017) analyzed the impact of detonation product leakage on fragment energy through numerical simulation. The results indicated that when detonation occurs at the center of the end face, leakage primarily occurs in the circumferential direction, significantly affecting the fragment's flight pattern.

Elek(2013), Backofen(1999), and others introduced the concept of two-stage shell acceleration by shock wave loading and detonation product loading through the analysis of experimental data. They derived the motion equation for the shell and an empirical formula for calculating the initial fragment velocity. The Gurney formula(1975) posits that all energy released during explosive detonation is converted into kinetic energy of the gas and shell; however, it only considers the effect of detonation product gas and neglects the influence of the detonation wave. Lindsay C m et al.(2010) proposed a data processing method based on the standard cylinder test, distinguishing and describing the driving effects of shock wave and detonation product gas expansion on the shell. They contended that the combined action of these two factors causes the shell to expand and accelerate. Building on this, Wang(2017) experimentally measured the expansion and acceleration process of a shell driven by internal explosive detonation, dividing shell motion into two processes: shock wave loading and detonation product loading, and fitting the corresponding curves.

In summary, this paper primarily investigates the influence of liners on the characteristics of fragments formed by prefabricated shell charge structures. Through experimental and numerical simulations, it examines prefabricated shell charge structures composed of 10# steel and 7075 aluminium liner materials. It analyzes the effect of different liner materials and thicknesses on explosion-driven fragmentation and gas leakage, and explores the influence law of liners on fragments.

2 Experimental Investigation on Detonation of Lined Semi-Prefabricated Shell Charge Structure

To investigate the influence of the liner on the velocity characteristics of fragments generated from a semi-prefabricated shell charge structure, the explosive experimental investigation of water recovery fragments was carried out under typical working conditions. The experimental setup is illustrated in Fig. 1 and Fig. 2. The velocity of the fragments was ascertained by analyzing the perforation on the witness target plate and utilizing velocity measuring target paper. The two witness targets were positioned 3m away from the charge structure, and the length, width and thickness of the witness target plate are 1.5m*1m*6mm respectively.

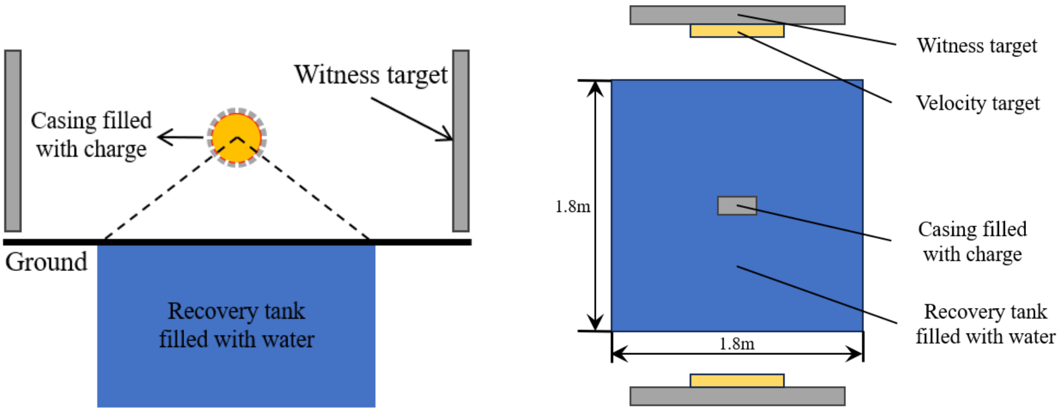

(a) side view (b) vertical view

Figure 1 *Schematic of experimental setup.*

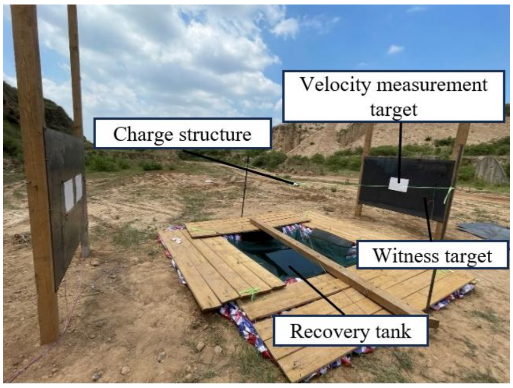

Figure 2 *Photo of experimental setup.*

Fig. 3. Shows the structure of the lined charge. The external diameter of the charge structure is 50 mm, with a length of 99 mm. The outer assembly is comprised of 12 identically stacked rings, 16 grooves uniformly distributed in the circumferential direction, which measuring 0.8 mm in width and 3.4 mm in depth. The thicknesses of the upper part and lower part liner sections are 1 mm and 1.5 mm. In the context of the two experimental iterations, the liner materials employed are 10# steel and 7075 aluminium alloy. The bottom thickness of the liner is 3 millimeters， additionally, a steel end plate, possessing a thickness of 3 millimeters, is positioned at the uppermost extremity of the charge structure, effectively mitigating the effect of axial rarefaction waves on the fragment velocity.

Figure 3 *Schematic and photos of experimental specimens.*

Table 1 Main material properties of 40Cr.

Density(g/cm³)	**Yield strength (MPa)**	**Elastic modulus(GPa)**	**Poisson's ratio**
7.87	785	211	0.3

Table 2 Main material properties of 10# steel.

Density(g/cm³)	**Yield strength (MPa)**	**Elastic modulus(GPa)**	**Elongation**
7.87	282	516	43%

Table 3 Main material properties of 7075 aluminium.

Density(g/cm³)	**Yield strength (MPa)**	**Elastic modulus(GPa)**	**Elongation**
2.8	420	74	31%

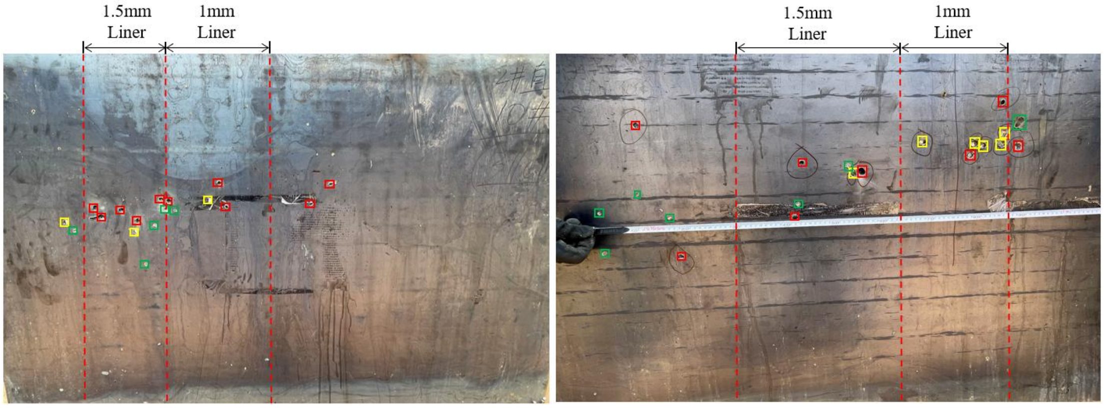

Figure 4 *Corresponding target of 10# steel lined warhead.*

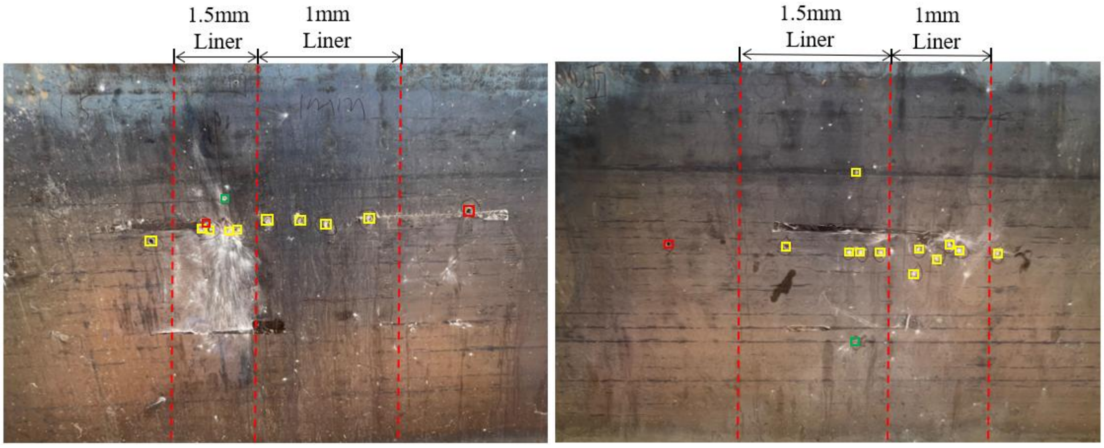

Figure 5 *Corresponding target of 7075 aluminium lined warhead.*

Note: Red corresponds to unperforated fragments, yellow indicates perforated fragments, and green signifies debris generated from liner fragmentation or fragment fracture.

Table 4 Statistical analysis of fragment penetration rates for various liner charge configurations following explosion tests.

	Penetration rate of 1mm liner charge structure	**Penetration rate of 1.5mm liner charge structure**
10# steel liner	50%	30%
7075 aluminium liner	100%	90%

Table 5 Measured fragment velocity in explosion test.

	Material	**Thickness**	**Filled ratio**	**Fragment velocity**
1	10# steel	1	0.415	1443
2	10# steel	1.5	0.361	1391
3	7075 aluminium	1	0.475	1470
4	7075 aluminium	1.5	0.435	1428

By the explosion testing of the lined semi-prefabricated shell charge configuration, the effect of the liner material on the power characteristics of fragments was investigated. Figs. 4 and 5 present the respective witness target of the explosion testing. 90% of the effective fragments were selected based on the fragment dispersion angle, specifically, those fragments located between the outermost two rows of red lines in Figs. 4 and 5 were subjected to detailed analysis and discussion. As evident from the figures, the count of fragments perforating of the 10# steel liner is markedly lower than that observed for the 7075 aluminium liner. Furthermore, the perforation count of fragments associated with the 1mm thick 10# steel liner exceeds that of fragments corresponding to the 1.5mm thick liner. Notably, only a single fragment from the 7075 aluminium liner corresponds to the fragment at the 1.5mm thick liner that failed to penetrate the target.

Through a explosion test of a semi-prefabricated cylindrical charge structure equipped with a liner, and based on the measurement results pertaining to target penetration and fragment velocity, we elucidated the influence laws of different liner materials and varying liner thicknesses on the fragment velocity of the charge structure. The findings indicate that the fragment velocity exhibited by the 7075 aluminium liner structure surpasses that of the 10# steel liner structure. Moreover, as the thickness of the liner increases, the fragment velocity of the charge structures composed of both materials experiences a decrement. Notably, the material composition and thickness of the liner exert distinct effects on the fragment velocity, with the thickness of the liner demonstrating a more significant influence on this parameter.

3 Numerical simulation investigation on explosion driving characteristics of liner to charge structure

3.1 Numerical simulation investigation on charge structure of semi-prefabricated shell with liner

For the explosion test of the aforementioned lined semi-prefabricated cylindrical shell charging structure, a comparative numerical simulation study was conducted under identical operational conditions to those of the test. The numerical simulation model and enlarged local grid of semi-prefabricated charge structure with liner are shown in Fig. 6.

In this study, the finite element software Autodyn, specialized for explosion and impact simulations, was employed to model the dynamic response behavior of the semi-prefabricated cylindrical shell with an inner liner subjected to internal explosion loading. Given that the maximum velocity fragments located in the circumferential middle section are unaffected by the sparse waves from both ends, the simulation was streamlined into a two-dimensional plane strain model. The ALE algorithm was utilized, wherein the Lagrange grid was applied to the shell and liner, the Euler grid to the explosive and air, and the "outflow" boundary condition was imposed on the air grid to preclude pressure reflection. The size of the charge structure in the numerical simulation is consistent with the test conditions, with a Lagrange grid size of 0.2 mm and an Euler grid size of 0.3 mm. Owing to the symmetry of the entire structure, and to more distinctly illustrate the expansion and broken processes of the liner and shell at typical time points, only a quarter of the model is presented.

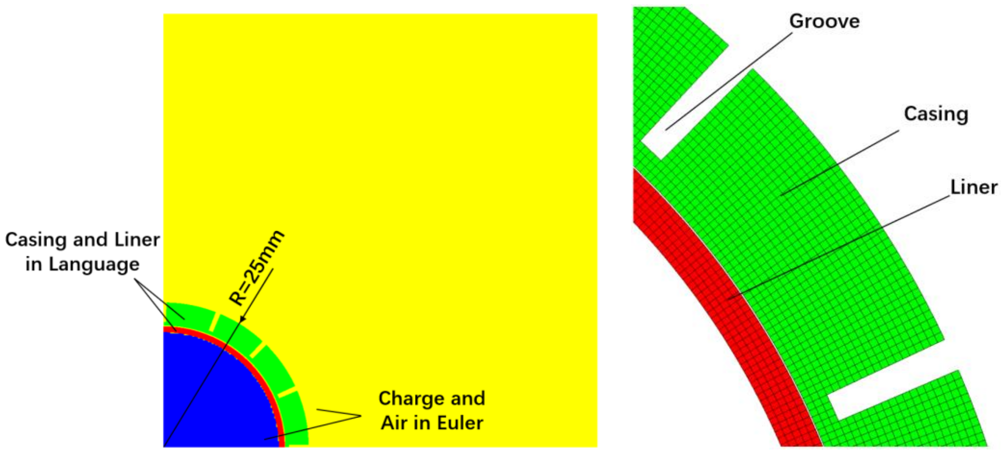

Figure 6 *Numerical simulation model and enlarged local grid of semi-prefabricated charge structure with liner.*

The shell is constructed from 40Cr material, with the J-C material model employed for its characterization. The liner is fabricated from 10# steel, while the Steinberg-Guinan model is adopted for the 7075 aluminium component. For the explosive material B, the JWL equation of state is selected. Detailed parameters pertaining to the shell, liner, and explosive can be found in Table 6-9.

Table 6 Main J-C model parameters of 40 Cr.

ρ(g/cm³)	A(MPa)	B(MPa)	C	N	M	T/(K)
7.87	905	226	0.03	0.21	0.83	1793

Table 7 Main J-C model parameters of 40 Cr.

ρ(g/cm³)	A(MPa)	B(MPa)	C	N	M	T/(K)
7.83	205	230	0.12	0.21	1.03	1793

Table 8 Main S-G model parameters of 7075 aluminium.

ρ(g/cm³)	N	T/(K)
2.8	0.1	1220

Table 9 Main parameters of JWL equation of state for explosive B.

ρ(g/cm³)	D(m/s)	P_{cj}(GPa)	E_0(kj/m³)	C_1(GPa)	C_2(GPa)	R1
17.15	7980	29.5	8.5	524	7.68	4.2

The explosion-driven process of the 1.5 mm-thick 10# steel liner charge configuration is comprehensively analyzed. The dynamic response behavior of both the liner and the semi-prefabricated shell subjected to explosion driving is illustrated in Fig. 7.

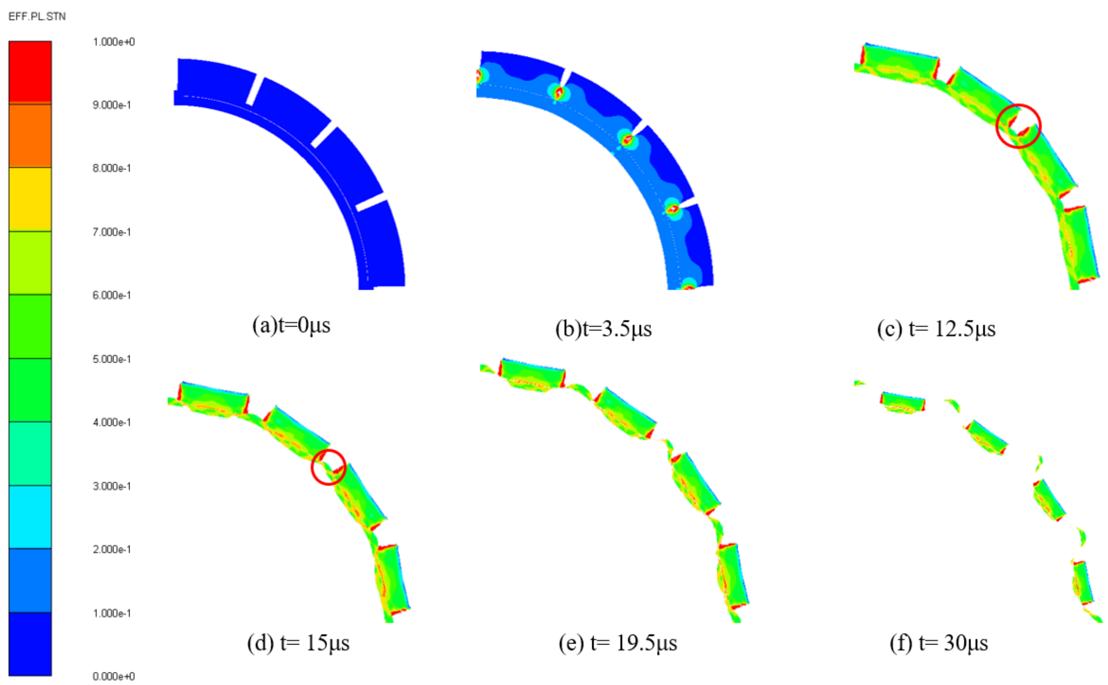

***Figure 7** Expansion and fracture process of typical semi-prefabricated shell with liner driven by detonation (1.5mm thick 10# steel liner).*

Following the initiation of the explosive, the liner and shell undergo outward expansion under the influence of the explosion shock wave. Upon transmission of the detonation wave, both the shell and the liner undergo deformation, with strain concentrating at the base of the grooves (Fig. 7b). The shell fractures at the bottom of each groove, and the fractured shell segments, along with the intact liner, expand outward in unison. As the shell continues to expand, the liner persists in expanding outward alongside the fragments, effectively preventing the leakage of detonation products (Figs. 7c and 7d). Between the fragments and the protruding sections of the liner, they persist in colliding and compressing against each other, resulting in the formation of localized strain bands (Figs. 7c and 7d). At the location of these strain bands, the liner initiates cracking (Fig. 7e), which progresses until the detonation gas is fully dissipated (Fig. 7f). Concurrently, it is evident that significant liner fragments are present under these operational conditions.

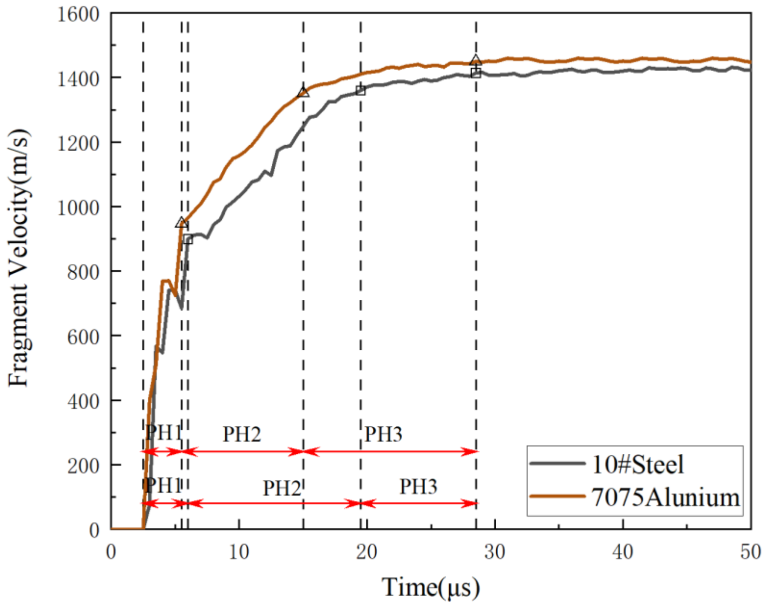

Figure 8 *Numerical simulation of the Time History Curve of Fragmentation Velocity for the Liner Charge Structure. (1.5mm thick liner)*

By integrating the dynamic fragmentation response processes of both the liner and the semi-prefabricated shell depicted in Fig. 7, we proceed to analyze the fragmentation acceleration process. Fig. 8 presents the time history curves of fragmentation velocity for the 10# steel liner and the 7075 aluminium liner charge structure. In the case of the 7075 aluminium-lined charge structure, upon initiation of the explosive charge, the detonation wave penetrates the shell at 2.5 μs, marking the onset of shell acceleration. An obvious upward trend in velocity is observed between 2.5 μs and 5.5 μs, which then gradually slowing down between 5.5 and 15 μs. At the 15 μs mark, the detonation products begin to leak out, further attenuating the acceleration of the fragments. Beyond 28.5 μs, the velocity stabilizes and remains essentially unchanged. The fragment acceleration process observed in the 10# steel liner exhibits similarities to that of the 7075 aluminium liner, only with distinct temporal action nodes.

Based on the characteristics of explosion-driven processes and the distinct acceleration patterns observed in the simulation curves of fragment velocity over time, the fragment acceleration can be delineated into three distinct stages: an initial shock wave-dominated stage, where the detonation wave propels the shell to rapidly accelerate within a brief period; a mid-term detonation product gas propulsion stage, characterized by a gradual deceleration of the acceleration effect over a relatively extended duration; and a later stage, which accounts for gas leakage following the rupture of the inner liner, leading to a further deceleration in the increase of shell velocity, as illustrated by the time axis of the explosion-driven action depicted in Fig. 9.

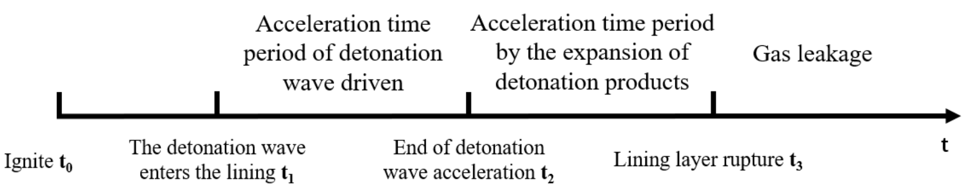

Figure 9 *Time axis of explosion driving process.*

Based on Fig. 7 and 8, it is evident that during the shock wave driving stage, the wave impedance of the aluminium liner is lower than that of the steel liner, leading to a faster detonation wave velocity. The energy consumed by the detonation wave during the driving process is relatively low, resulting in a higher fragment velocity at this stage, attributed to the inherently low density of aluminium. In the gas propulsion stage, the gas leakage radius of the 10# steel liner is notably large, and as a result, the 10# steel liner structure attains a higher fragmentation velocity. During the gas leakage stage following the rupture of the inner liner, 7075 aluminium demonstrates a smaller gas leakage radius. This leads to a large pressure difference between the interior and exterior upon rupture of the inner liner, enabling the fragments to achieve greater velocities. Under the combined influence of these three stages, the aluminium liner structure exhibits a significantly greater fragmentation velocity.

The fragment velocity obtained through numerical simulation is 1409 m/s, while the experimentally measured fragment velocity is 1391 m/s, which matched well. Figures 10 and 11 and Table 10 present a comparative analysis between the fragments retrieved from the experimental tests and those generated by the simulation. The dimensions of the recovered fragments exhibit a high degree of concordance with the simulation results, thereby validating the feasibility of the simulation approach. Fig. 12 illustrates the corresponding liner fragments that were successfully retrieved.

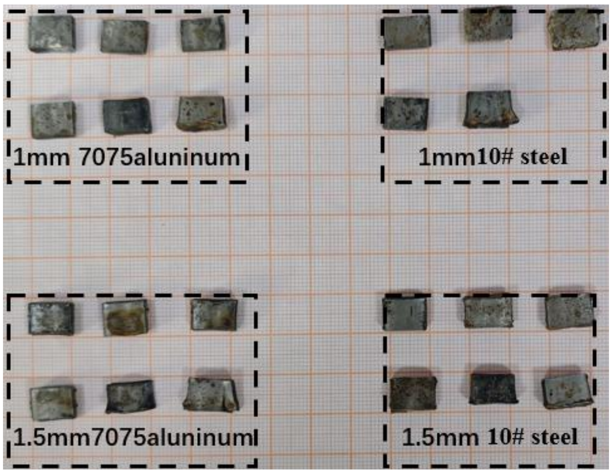

Figure 10 *Experimental recovery of some fragments.*

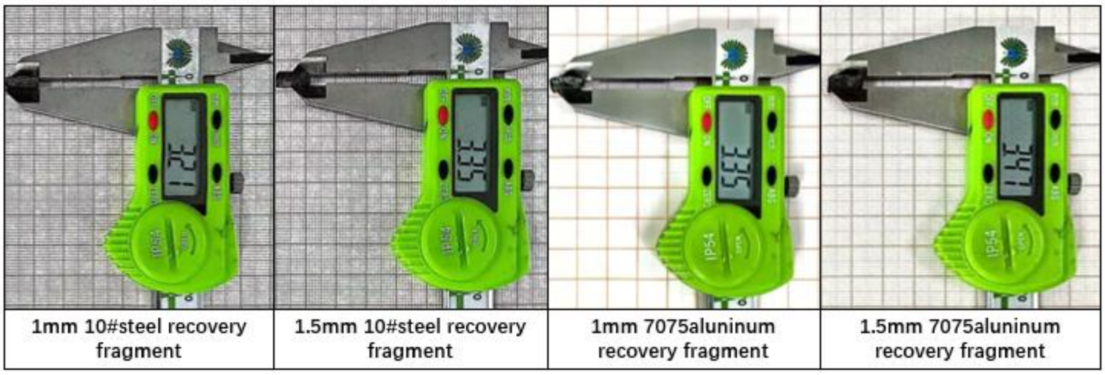

Figure 11 *Comparison of recovered fragments and Simulation of 10# steel liner charge structure test.*

Table 10 Numerical simulation calculation of fragment thickness

Material	Thickness of liner(mm)	Thickness of fragment(mm)
10# steel	1	3.13
	1.5	3.21
7075 aluminum	1	3.25
	1.5	3.38

(a) 7075 aluminium liner trace.(b) 10# steel liner debris.

Figure 12 *Comparison of recovered fragments and Simulation of 7075 aluminium lined charge structure test (1.5mm thick).*

According to the comparison between the numerical simulation results and the experimental recovery results, it can be seen that the maximum error between the fragment thickness of the 1mm thick 10 # lining charge structure recovered from the experiment and the numerical simulation is 3.5%, the minimum error is 1.2%, and the average error is 2.6%. The maximum error between the fragment thickness of the 1.5mm thick 10 # lining charge structure and the numerical simulation is 5.6%, the minimum error is 3.1%, and the average error is 4.4%; The maximum error between the fragment thickness of the 1mm thick 7075 aluminum alloy lining charge structure and numerical simulation is 3.7%, the minimum error is 2.2%, and the average error is 2.7%. The maximum error between the fragment thickness of the 1.5mm thick 7075 aluminum alloy lining charge structure and numerical simulation is 4.2%, the minimum error is 1.5%, and the average error is 2.8%.

Based on a simulation study of the lined semi-prefabricated cylindrical charge structure under identical test conditions, the dynamic crushing response characteristics of this structure, driven by detonation, were elucidated. Through the analysis of the fragment velocity-time history curves obtained the staged acceleration characteristics of fragments. A comparison between experimental and simulation results revealed a close correspondence in fragment velocity, and the recovered fragment sizes were in excellent agreement with the simulation predictions, thereby substantiating the feasibility and reliability of the simulation approach.

3.2 Investigation on the influence of liner on the velocity of semi-prefabricated fragments

In the subsequent analysis, the influence of different liner thickness and different liner materials on fragment velocity under the same charge structure caliber is studied by simulation. To assess the influence exerted by the liner when driven by an identical charge, simulation studies were conducted utilizing a uniform charge size. Specifically, simulation models were established for charge structures with a 50mm diameter, encompassing various liner materials and thicknesses. Additionally, simulation models for different liner materials and thicknesses were developed under the condition of a 40mm inner diameter explosive charge, aiming to delve into the effect of the liner on the velocity of semi-prefabricated fragments. The shell structure remained consistent with the previous configuration, and the simulation outcomes are presented in Fig. 13 and Fig. 14.

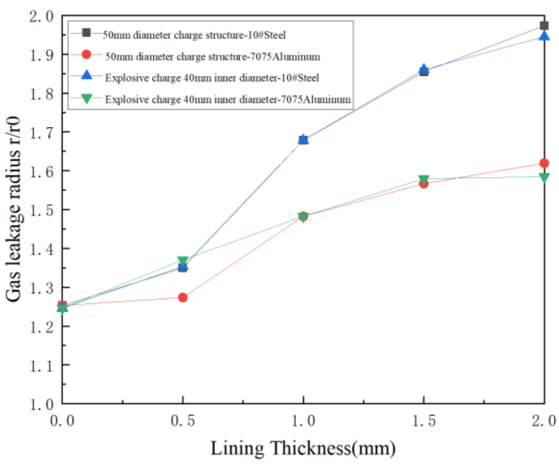

Figure 13 *Numerical simulation curves of gas leakage radius and liner material and thickness.*

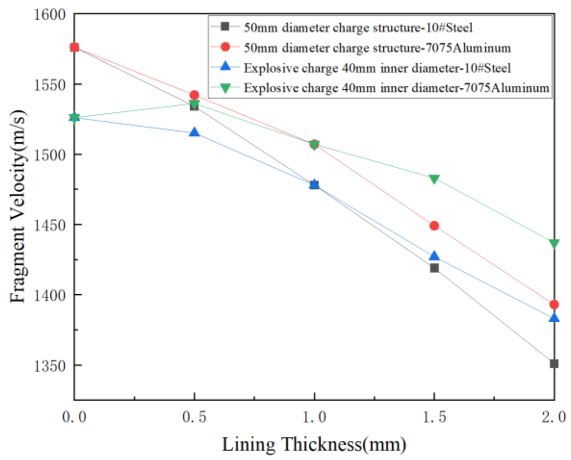

Figure 14 *Numerical simulation curves of fragment velocity and liner material and thickness.*

Fig. 13 and Fig. 14 present the simulation curves illustrating the variation of fragment velocity and gas leakage radius with respect to material and thickness, respectively. It is evident from these figures that, given the same thickness, the gas leakage radius of the 10# steel-lined charge structure exceeds that of the 7075 aluminium liner. As the thickness of the liner increases, so does the gas leakage radius. Referring to the dynamic expansion characteristics of the semi-prefabricated charge structure with liner previously discussed (Figure 7(e)), it can be observed that the outer shell ruptures prior to the inner liner. As the shell and liner continue to expand, the inner liner undergoes stress concentration and subsequently fractures. Owing to the lower strength of 7075 aluminium compared to 10# steel, the 7075 aluminium liner reaches its failure threshold first at the location of stress concentration, leading to the formation of cracks and ultimate macroscopic fracture. This results in a larger gas leakage radius under the 10# steel liner structure. Furthermore, as the thickness of the liner increases, the duration for crack propagation elongates, delaying the time and location of macroscopic fracture of the liner, and consequently, augmenting the radius of gas leakage.

Under identical liner thickness conditions, the fragmentation velocity of the 7075 aluminium liner structure surpasses that of the 10# steel liner, and this velocity differential widens as the liner thickness increases. When pertains to a 50mm caliber charge structure, an increase in wall thickness leads to a reduction in charge mass and driving capability, consequently resulting in a decrease in fragment velocity. When the working condition involves the same explosive charge with an inner diameter of 40mm, the driving capability of the charge remains consistent, only the fragment velocity of the 0.5mm aluminium liner exceeds that of the unlined fragment, while the fragment velocities observed in all other working conditions are lower compared to the unlined fragment velocity.

In conclusion, metal materials with superior strength as the liner can enhance the gas leakage radius of the liner, prolong the gas leakage duration of detonation products, and amplify the propulsive effect exerted by detonation products on fragments. Nevertheless, the augmentation of the gas leakage radius solely yields benefits during the pushing stage preceding the gas leakage of explosion-driven products. The imparting of fragment velocity must also account for the influence of the shock wave, as the liner thickness increases, the kinetic energy acquired by the shell under the impact of the shock wave diminishes, exerting a detrimental effect on the elevation of fragment velocity. Consequently, for the lined semi-prefabricated charge structure under the operational conditions examined in this section, 7075 aluminium is more appropriate for utilization as the liner material of the charge structure compared to 10# steel.

3.3 Study on the influence of liner on the velocity of fully prefabricated column fragments

To investigate the influence of liner on the power characteristics of fragments in a fully prefabricated column fragment charge structure, a model of fully prefabricated column fragment charge structure with liner as established, as illustrated in Fig. 15. In this structure, the fragments have a diameter of 5 mm, and 24 fragments are uniformly distributed along the circumferential direction, without considering the issues related to accumulation.

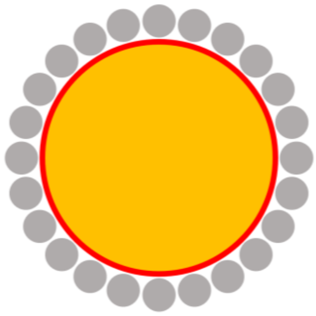

Figure 15 *Schematic of liner fully prefabricated column fragment structure.*

(1) Investigation on the dynamic crushing response process of a fully prefabricated column fragment charge with liner

The explosion-driven process of the charge structure with a 1.5 mm thick 10# steel liner is examined. The dynamic response behavior of both the liner and the column fragments under explosion driving is depicted in Fig. 17.

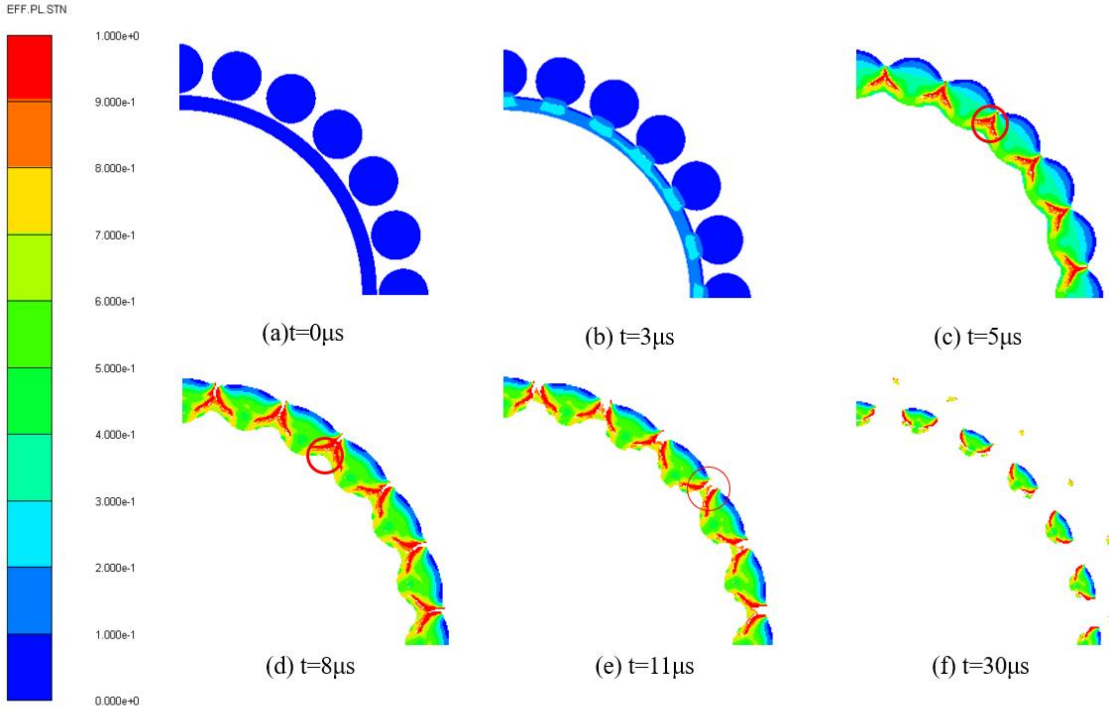

Figure 16 *Explosion driven expansion and fragmentation process of typical fully prefabricated column fragments of liner (1.5mm thick 10# steel liner).*

Upon detonation of the explosive, the liner expands outward under the influence of the explosion shock wave. Following the introduction of the detonation wave, the liner collides and compresses the column fragments (Fig. 16b), resulting in deformation of the liner at the point of collision. As the liner continues to expand, the fragments are deformed into an ellipsoidal shape, and the liner undergoes significant deformation. The column fragments experience compression in the circumferential direction and, in conjunction with the liner, close off the gas leakage channel (Fig. 16c). Subsequently, the liner fractures irregularly at the gap, and the detonation product gas begins to leak (Fig. 16d and Fig. 16e).

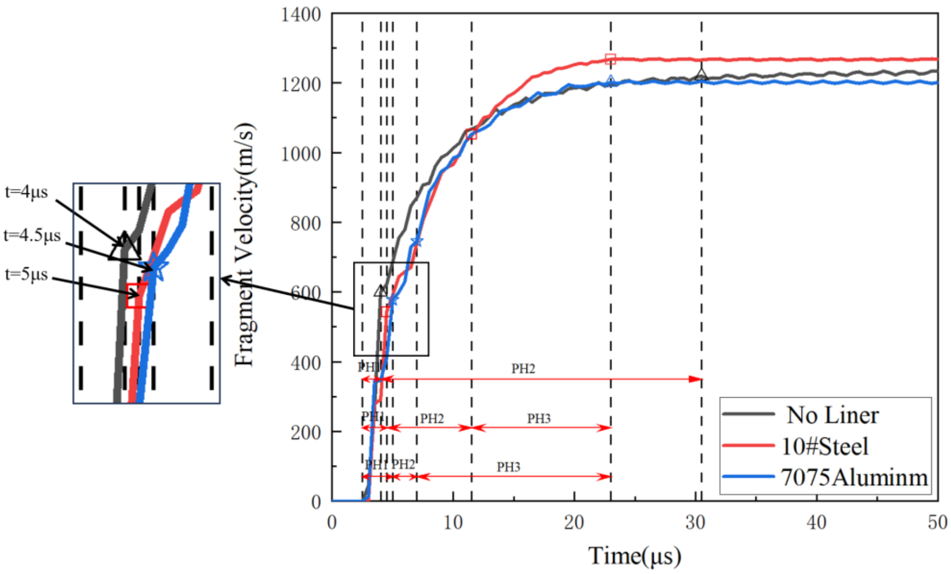

Figure 17 *Simulation curvse of fragment velocity time history of fully prefabricated charge structure.*

Note: The unlined charge structure has only two different acceleration stages during fragment acceleration due to direct gas leakage of detonation products.

Based on the time axis of the detonation driving action depicted in Figure 9, and the dynamic fragmentation response process of the liner and fully prefabricated fragments illustrated in Figure 16, an analysis of the fragment acceleration process is conducted. Figure 17 presents the velocity-time history curves of fragments under the fully prefabricated charge structure. For the 10# steel liner charge structure, upon ignite of the charge, the detonation wave reaches the liner at 2.5 μs, initiating their acceleration. The velocity experiences a significant increase between 2.5 and 5 μs, followed by a gradual slowing of the upward trend in fragment velocity from 5 to 11 μs. At 11 μs, the detonation products of the liner leak out, further decelerating the fragment acceleration. After 23 μs, the velocity remains essentially unchanged. The fragment acceleration process for the 7075 aluminium liner exhibits similarities to that of the 10# steel liner, albeit with differing time action nodes. In the case of the unlined charge structure, the detonation products leak directly, and following the acceleration stage dominated by shock wave driving, it transitions directly to the acceleration stage influenced by gas leakage. As demonstrated in Figure 17, the unlined charge structure exerts a significantly longer influence on fragment driving time during the gas leakage stage compared to the lined charge structure.

When the charge structure is unlined, the detonation wave directly acts on the fragments, which can maximize the use of the energy of the shock wave. However, the detonation product gas produced by the explosion leaks directly from the gaps between the fragments, resulting in a low energy utilization rate for driving the acceleration of the fragments, leading to a lower velocity of the fully prefabricated fragments without lining. Conversely, when the overall charge structure incorporates an inner liner, the shock wave enters the fragments through the inner lining, thereby minimizing the dissipation of shock wave energy into the air. Simultaneously, the inner liner delays the leakage of detonation product gas and increases the utilization rate of detonation product gas energy.

(2) Investigation on the influence of liner on the velocity of fully prefabricated column fragments

A simulation study is presented to investigate the effects of varying liner thickness and liner materials on fragment velocity within a 50 mm diameter charge structure, as well as their influence on fragment velocity under a 40 mm inner diameter of the same explosive charge. The charge structure remains consistent with the previous configuration, and the simulation outcomes are illustrated in Figs. 18-20.

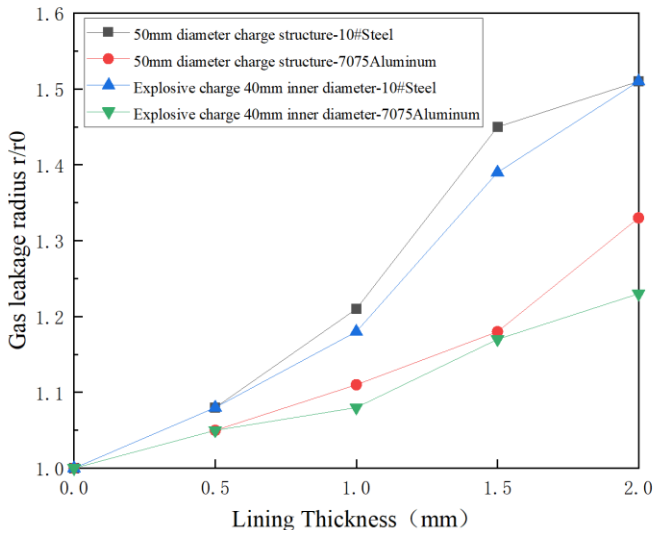

Figure 18 *Relation curve between gas leakage radius and liner material and thickness.*

When the thickness of the liner is less than 1 mm, the gas leakage radius for the two liner materials within the charge structure is quite small, with no significant difference observed. However, when the inner liner thickness reaches or exceeds 1 mm, a marked difference in the gas leakage radius becomes apparent between the two materials. As the thickness of the inner liner increases, the gas leakage radius under the 10# steel liner surges dramatically, whereas the increase under the 7075 aluminium liner is more gradual. At a liner thickness of 0.5 mm, both materials' inner liners rupture directly under the detonation effect, allowing the detonation product gas to leak directly through the gaps between the fragments. When the thickness is 1 mm, the 7075 aluminium liner reaches its failure threshold and cracks upon collision with the fragments. This results in a significant delay in gas leakage for the 10# steel liner, but the delay effect for the 7075 aluminium liner is not clearly. For liners with a thickness of 1 mm or greater, the process of delaying gas leakage differs between the two liner materials. As illustrated in Figure 19, when the deformation and compression of the column fragments in the circumferential direction, combined with the liner, act to delay the leakage of detonation product gas, the aluminium liner cracks prematurely due to its lower strength. As the fragments and liner continue to expand until the column fragments separate in the circumferential direction, the detonation product gas in the aluminium-lined charge structure leaks directly. In contrast, the steel liner continues to delay gas leakage effectively until it eventually fractures. It is worth noting that in the absence of an inner liner within the structure, the detonation product gas leaks directly through the gaps between the fragments.

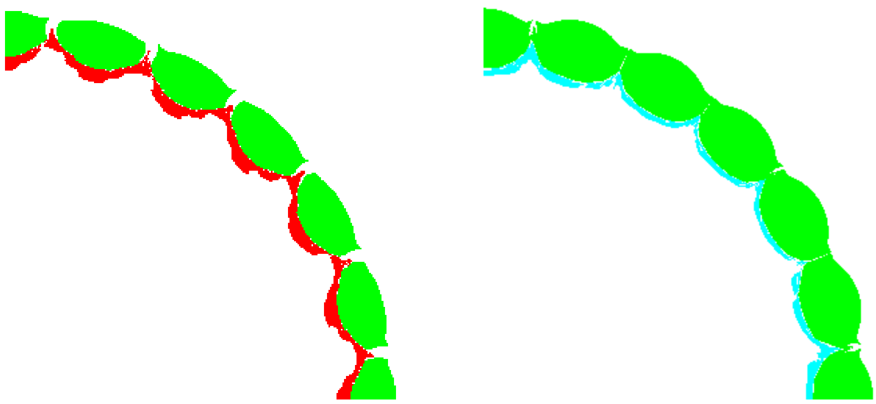

(a) 10# Steel liner (10μs) (b) 7075 Aluminium liner (7μs)

Figure 19 *Liner and fragment structure of 1.5mm thick different materials during explosion driving.*

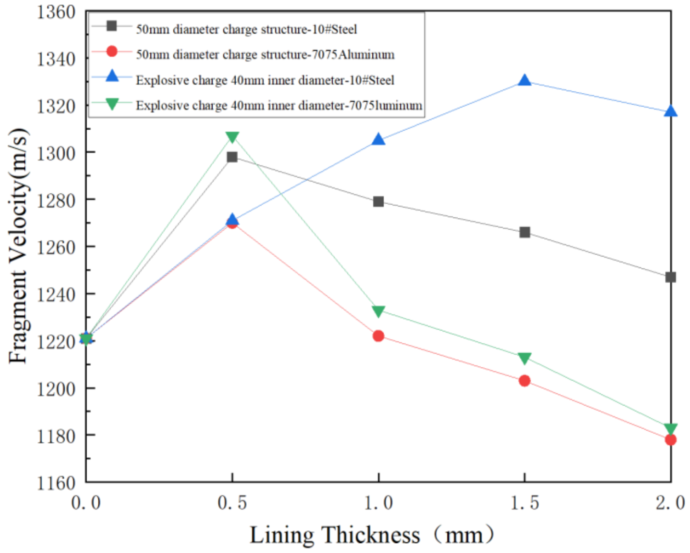

***Figure 20** Relation curve between liner material, thickness and fragment velocity.*

Fig. 20 presents the simulation curve illustrating the relationship between fragment velocity and both the material and thickness of the liner. In the absence of a liner in the charge structure, the fragment velocity is observed to be low. However, as the liner thickness increases, the fragment velocity exhibits an initial increase followed by a subsequent decrease. Under identical conditions, and with the liner thickness held constant, the velocity of fragments from the 10# steel liner is found to be higher than that of the 7075 aluminium liner.

When the liner material is composed of 7075 aluminium, the trend observed in the relationship curve between fragment velocity and liner thickness remains consistent for both the 50mm caliber charge structure and the explosive charge with a 40mm inner diameter. The fragment velocity reaches its peak with a 0.5mm thick liner structure, exhibiting an approximate 7% increase compared to the unlined configuration. Similarly, when 10# steel is used as the liner material in the 50mm caliber charge structure, the maximum fragment velocity is attained with a 0.5mm thick liner, resulting in an approximate 6.3% increase in fragment velocity relative to the unlined structure. Furthermore, under the same explosive charge conditions with a 40mm inner diameter, the optimal fragmentation velocity is achieved with a 1.5mm thick inner liner, yielding an approximate 8.9% increase in fragmentation velocity compared to the case without liner.

In the process of explosion-driven fully prefabricated column fragments with a liner, the material of the liner exerts a more notable influence on the velocity of the fragments than does its thickness. When subjected to the inner liner composed of two different materials, fully prefabricated column fragments experience distinct acceleration process during explosion driving. The steel liner possesses greater strength compared to the aluminium liner, which enables the charge structure to have a larger gas leakage radius. Consequently, under the conditions discussed in this section, the fragment velocity of a steel liner of the same thickness exceeds that of an aluminium liner. As the thickness of the inner liner increases, the continual increase in liner thickness alters the energy distribution between the shell and the liner layer. The energy of the shock wave is increasingly converted into the internal energy of both components and the kinetic energy of the liner. During the shock wave driving phase, an increase in liner thickness leads to a decrease in fragment velocity. The gas leakage radius of the fully prefabricated column fragment charge structure with a liner is significantly smaller than that of the semi-prefabricated shell charge structure with a liner, and the leakage occurs earlier. Therefore, the contribution of the liner to the fragment velocity of the fully prefabricated charge structure during the detonation product propulsion stage is relatively modest.

To conclude, in the context of the fully prefabricated column fragment charge structure, the liner serves to enhance both fragment velocity and gas leakage radius. When comparing fragment velocities, it is evident that the aluminium liner can effectuate an increase of approximate 7%, whereas the steel liner can elevate the velocity by a maximum of approximate 8.9% relative to the unlined configuration. Furthermore, when juxtaposing the influence of liner thickness against that of liner material, it becomes apparent that the latter is the predominant factor governing fragment acceleration. Under the operational parameters pertinent to this section, the 10# steel liner emerges as the optimal choice for the charge structure's liner.

4 Conclusion

To investigate the influnce of liner on the fragmentation performance characteristics of charge structures, both explosion tests and numerical simulation studies were carried out on semi-prefabricated charge structures with liner. Additionally, numerical simulation studies were conducted on fully prefabricated column fragment charge structures with liner. The dynamic behaviors, gas leakage patterns, and fragment velocity profiles of the liner and shell were compared across different materials and thicknesses. The primary conclusions are as follows:

(1) The influence of liner material and thickness on the fragmentation velocity of semi-prefabricated charge structures with liner was found out through explosion tests. Under the specific conditions examined in this article, it was found that the fragmentation velocity of the charge structure lined with 7075 aluminium exceeded that of the structure lined with 10# steel. Furthermore, the fragmentation velocity decreased as the liner thickness increased. For semi-prefabricated propellant structures with liner, the thickness of the liner exerted a more significant effect on fragment velocity compared to the liner material itself.

(2) Based on the numerical simulation of the semi-prefabricated shell charge structure incorporating a liner, the dynamic expansion and fragmentation processes of both the liner and the shell under explosion driving were elucidated. It was observed that the liner fractured subsequent to the shell, effectively delaying the gas leakage of detonation products. By analysing the velocity-time history curves of the charge structure, the three-stage acceleration characteristics, spanning from the explosion-driven semi-prefabricated shell with liner to the formation of fragments, were identified. Furthermore, the influence of the liner on the charge structure of the semi-prefabricated shell was clearly demonstrated.

(3) Through a comparative analysis of numerical simulations of semi-prefabricated shell charges featuring various liner materials and thicknesses, it was revealed that, for a given liner material, an increase in liner thickness results in an enlarged gas leakage radius and a reduced fragment velocity. When the liner thickness remains constant, different liner materials exert distinct influences on the gas leakage radius, with the fragmentation velocity of the 7075 aluminium liner surpassing that of the 10# steel liner.

(4) By numerical simulation studies on the fully prefabricated column fragment charge structure incorporating a liner, the dynamic response characteristics of both the liner and fragments under explosion driving were elucidated. By integrating velocity-time history curve analysis, the acceleration characteristics of the fully prefabricated fragment charge structure subjected to explosion driving were derived. Furthermore, the influence of the liner on the fully prefabricated fragment charge structure was clearly demonstrated.

(5) Through a comparative analysis of numerical simulations of fully prefabricated fragment charge structures featuring different liner materials and thicknesses, it was discovered that the incorporation of a liner enhances both the gas leakage radius and fragment velocity of the charge structure. As the thickness of a given liner material increases, the gas leakage radius expands, and the fragment velocity initially rises before subsequently decliner. When the inner liner thickness remains constant, the 10# steel liner exhibits a larger gas leakage radius and fragment velocity compared to other materials. In comparison to the unlined scenario, steel liner induces a more pronounced increase in fragment velocity than aluminium liner, with an approximate 10% enhancement. In the context of fully prefabricated column fragment charge structures with liner, the material of the liner exerts a more significant influence on fragment velocity than the thickness of the liner.

Acknowledgments

This study was partially supported by the National Natural Science Foundation of China (NSFC) (Grant No. 12472364). The authors would like to gratefully acknowledge this support.

Author's Contribuitions: Conceptualization, Yongnan Li and Yongxiang Dong; Methodology, Yongnan Li; Investigation, Yongnan Li and Wang Yao; Writing - original draft, Yongnan Li; Writing - review & editing, Peizhuo Shi and Yujing Li; Resources, Yongxiang Dong and Zhiyu Shao; Supervision, Yongxiang Dong.

Editor: Rogério José Marczak

References

Taylor, G. I. (1963). The fragmentation of tubular bombs. In Scientific Papers of G. I. Taylor (Vol. 3, p. 387). Cambridge University Press.

Hoggatt, C. R., & Recht, R. F. (1968). Fracture behavior of tubular bombs. Journal of Applied Physics, 39, 1856–1862.

Zhang, S. Z., & Sun, Y. B. (1985). Deformation and rupture of rigid-plastic cylinder shell due to explosion. ACTA Armamentarii, 2, 59–65.

Hutchinson, M. D., & Price, D. W. (2014). On the continued acceleration of bomb casing fragments following casing fracture. Defence Technology, 10(2), 211–218.

Zhou, M., Wu, C., An, F., et al. (2020). Acceleration characteristics of discrete fragments generated from explosively-driven cylindrical metal shells. Materials, 13(9), 2066.

Yin, L. Q., Jiang, J. W., Men, J. B., et al. (2014). Calculation model of initial velocity of cubic prefabricated fragment warhead fragments [Original work in Chinese]. Acta Armamentarii.

Li, Y., Li, Y. H., & Liu, C. (2017). Numerical simulation of detonation product leakage in prefabricated fragment warheads [Original work in Chinese]. Journal of Beijing Institute of Technology, 37(8), 785–789.

Predrag, E., Slobodan, J., & Dejan, M. (2013). Modeling of the metal cylinder acceleration under explosive loading. Scientific Technical Review, 63(2), 39–46.

Backofen, J. E., & Weickert, C. (1999). Initial free-surface velocities imparted by grazing detonation waves. In M. D. Furnish, L. C. Chhabildas, & R. S. Hixon (Eds.), Shock Compression of Condensed Matter (pp. 919–922). American Institute of Physics.

Karpp, R. R., & Predebon, W. W. (1975). Calculations of fragment velocities from naturally fragmenting munitions. Ballistic Research Laboratories.

Lindsay, C. M., Butler, G. C., Rumchik, C. G., et al. (2010). Increasing the utility of the copper cylinder expansion test. Propellants, Explosives, Pyrotechnics, 35(5), 433–439.

Wang, X. Y. (2017). Research on several issues of energy conversion from explosive detonation to damage load [Unpublished doctoral dissertation]. Beijing Institute of Technology.